Minimizing Angular Error (AE) in 2D magnetic sensors by Non-Orthogonality Correction

Introduction

Magnetic sensors can be used for rotation detection. For this, usually a small magnet is attached to a shaft (or any other rotational axis). Thus, when the shaft rotates, the magnetic sensor will detect the change of the magnetic field orientation. Such magnetic sensors are also called 2D magnetic sensors.

The main component of our 2D magnetic sensors are based on arrays of magnetic tunnel junction (MTJ) cells (see Figure 1). Each MTJ cell is mainly composed by: 1) a pinned layer (PL) where the magnetization of such layer is fixed, 2) a sense layer (SL) where its magnetization can easily be oriented along the direction of the applied magnetic field and 3) a tunnel barrier between both PL and SL.

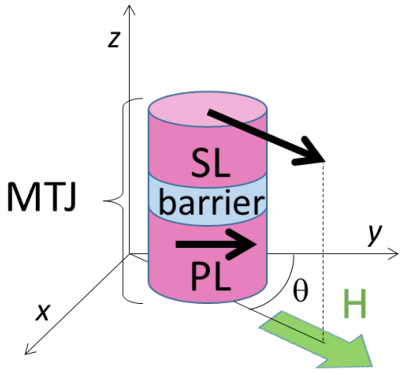

Figure 1: Schematic of a MTJ cell under the effect of an external magnetic field H.

The resistance R of each MTJ cell is dependent on the relative orientation θ between PL magnetization and SL magnetization due to the Tunneling Magneto-Resistance (TMR) effect:

$$R(\theta) = \frac{1}{G(\theta)} = \frac{1}{G_0 + \Delta G \cdot cos\theta} \qquad Eq\ (1)$$

Where G is the conductivity, ΔG is the change of conductivity due to the TMR effect and G_0 is the average conductivity between parallel and antiparallel configuration of the MTJ structure.

Thus, by changing the orientation of the applied magnetic field a variation of the output voltage is obtained.

A Wheatstone bridge architecture (see Figure 2) enables to obtain an output voltage V_{OUT} that is proportional to a sinusoidal signal with respect to θ. For this, each branch of the Wheatstone bridge consists of an array of MTJ dots connected in series and/or parallel. The orientation of the PL (arrows in Figure 2) is similar for diagonal branches (R1 and R4 or R2 and R3 in Figure 2) and opposite for those branches constituting a half bridge (R1 and R2 or R3 and R4 in Figure 1). Considering this:

$$\frac{V_{OUT}}{V_{DD}} = \left(\frac{R_2(\theta)}{R_1(\theta) + R_2(\theta)} - \frac{R_4(\theta)}{R_3(\theta) + R_4(\theta)}\right) \qquad Eq(2)$$

where V_{DD} is the applied voltage. Therefore, if all branches have similar resistances and considering Eq.1, V_{OUT} can be written as:

$$\frac{V_{OUT}}{V_{DD}} = \left(\frac{TMR}{TMR + 2}\right) \cdot cos\theta \qquad Eq\ (3)$$

In order to ensure, however, an unambiguous determination of θ, 2D sensors are usually based on two Wheatstone bridges where the orientation of the PLs are mutually orthogonal. By this configuration, two voltage outputs V_{SIN} and V_{COS} are generated by the 2D sensor, where V_{COS} follows a cosine (COS) signal and V_{SIN} follows a sine (SIN) signal (see Figure

2). Thus, the measured angle θ_{meas} will be determined by the arc tangent of the ratio between both signals:

$$\theta_{meas} = arctan\left(\frac{V_{SIN}}{V_{COS}}\right) \qquad Eq\ (4)$$

and Angular Error (AE) is the parameter that determines the accuracy of the measured angle θ_{meas}:

$$AE = \theta_{meas} - \theta \qquad Eq\ (5)$$

Several factors can lead however to a significant AE. One of the issues that is addressed in this application is the parameter dependence of AE, as well as different correction approaches that can be considered in order to mitigate their impact on AE.

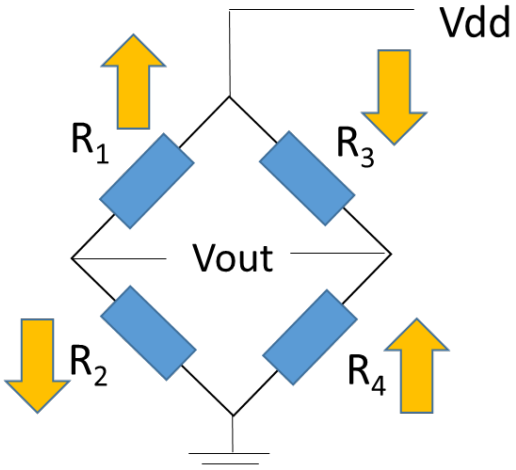

Figure 2: Schematic of a Wheatstone bridge architecture with 4 MTJ branches. Arrows show the orientation of the PL for each MTJ branch.

Parameter Dependence of AE

The output voltage of a 2D magnetic sensor with two (2) Wheatstone bridges can generally be written as:

$$V_{COS} = [A_{COS} \cdot cos(\theta + \alpha_{COS}) + C_{COS}] \qquad Eq\ (6a)$$

$$V_{SIN} = [A_{SIN} \cdot sin(\theta + \alpha_{SIN}) + C_{SIN}] \qquad Eq\ (6b)$$

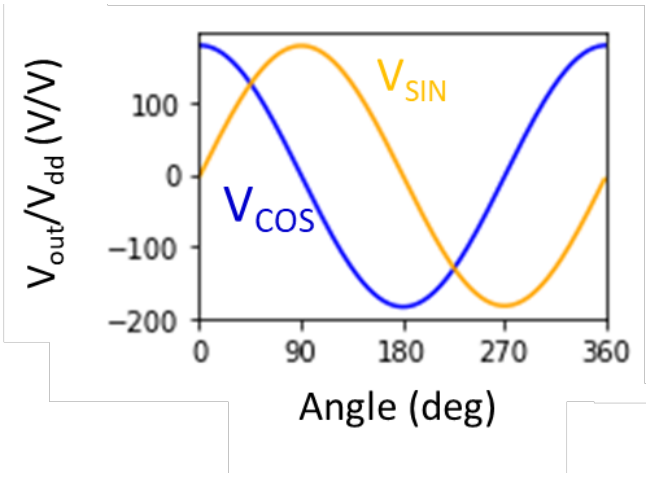

Figure 3: Typical angular dependence of the output voltage of a 2D magnetic sensor with two Wheatstone bridges, one orthogonally oriented with respect to the other.

Where A_{COS}, A_{SIN} are the amplitude, C_{COS}, C_{SIN} are the offset and α_{COS}, α_{SIN} are the phase shift of both COS and SIN bridges. Note that both amplitudes and offsets are now normalized parameters with respect to the applied voltage V_{DD} so V_{COS} and V_{SIN} can be expressed in mV/V.

Ideally, if both bridges present no offset (C_{COS} = C_{SIN} = 0), no phase shift (α_{COS} = α_{SIN} = 0) and their amplitudes are the same (A_{COS} = A_{SIN}), AE = 0. Any situation different from this would lead to an AE ≠ 0.

Figures 4, 5 and 6 summarizes the impact on AE for such parameters. Figure 4 shows how AE increases with both amplitude changes (ΔA_{COS}, ΔA_{SIN}) while Figure 5 and 6 shows how AE increases with offset changes and phase shift changes, respectively. In all three figures, normalized output voltages (V_{COS}/A_{COS} and V_{SIN}/A_{SIN}) are considered so Eq. 6a and 6b becomes:

$$v_{COS} = cos(\theta + \alpha_{COS}) + (C_{COS}/A_{COS}) \qquad Eq\ (7a)$$

$$v_{SIN} = sin(\theta + \alpha_{SIN}) + (C_{SIN}/A_{SIN}) \qquad Eq\ (7b)$$

Initial conditions are with no offset (C_{COS} = C_{SIN} = 0) nor any phase shift (α_{COS} = α_{SIN} = 0) as for an ideal

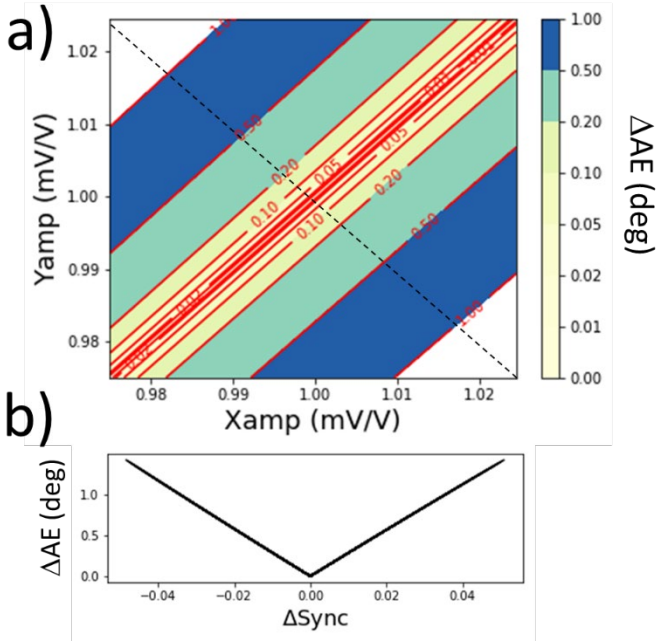

Figure 4: a) Increase of AE due to amplitude increase on both bridges. ΔXamp and ΔYamp are the variation ratio of both amplitude voltages. Dashed lines show increase of Sync direction. b) ΔAE vs. ΔSync.

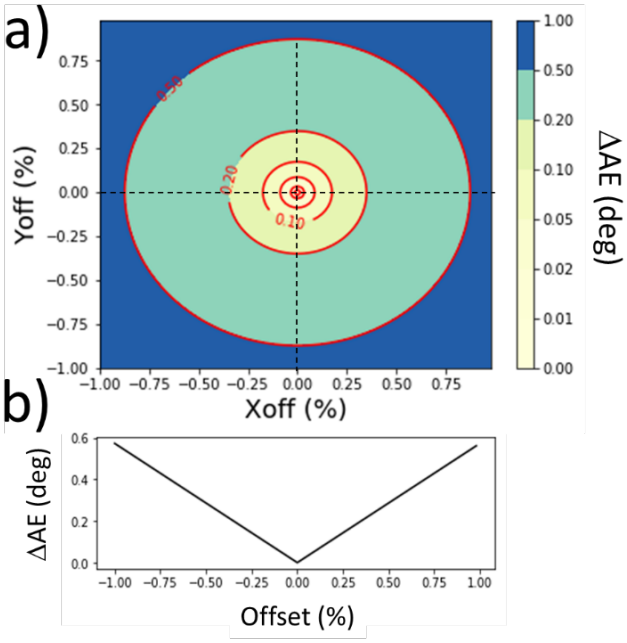

Figure 5: a) Increase of AE due to offset increase on both bridges. ΔXoff and ΔYoff are the variation ratio of both offset voltages b) ΔAE vs. ΔTotal Offset.

2D sensor. Changes in amplitudes and offsets can therefore expressed in percentage (%) with respect to their initial amplitudes A_{COS} and A_{SIN}. Dashed lines on Figures 5a, 6a and 7a show the direction of variation of synchronism (Sync = A_{COS}/A_{SIN}), total offset (C = $\sqrt{C_{COS}^2 + C_{SIN}^2}$), and non-orthogonality (Non-Orth) between both bridges. As we can see from these figures, those are the real parameters that determine AE.

Figures 4b, 5b and 6b plots the variation of AE vs. Sync, total offset, and Non-Orth respectively. In all three cases ΔAE is linear with respect to their variation (see Table I for summary of such variations).

Note also, that the harmonic contributions to the AE are not the same for all three parameters (see Table I). Figure 7 shows the angular dependence of AE for all three cases: a) Sync ≠ 1 (AE_{Sync}), b) Offset ≠ 0 (AE_{Off}) and c) non-orthogonality ≠ 0 (AE_{Orth}). As we can observe, mismatch amplitude (Figure 8a) and phase shift (Figure 7c) induce each of them an AE with a periodicity of π (2nd harmonic) while offset contributions induce an AE with a periodicity of 2π (1st harmonic). Each contribution to the AE could therefore be expressed as:

$$AE_{Sync} = AE_{Sync}^{0} \cdot sin(2\theta) \qquad Eq(A)$$

$$AE_{Off} = -AE_{Off}^{0} \cdot sin(\theta - \varphi) \qquad Eq(B)$$

$$AE_{Orth} = AE_{Orth}^{0} \cdot [1 + cos(2\theta)] \qquad Eq(C)$$

Where AE_{Sync}^{0}, AE_{Off}^{0} and AE_{Orth}^{0} are the slopes of Figure 4b, Figure 5b and Figure 6b respectively which values are shown in Table 1 and φ = arctan(C_{SIN}/C_{COS}).

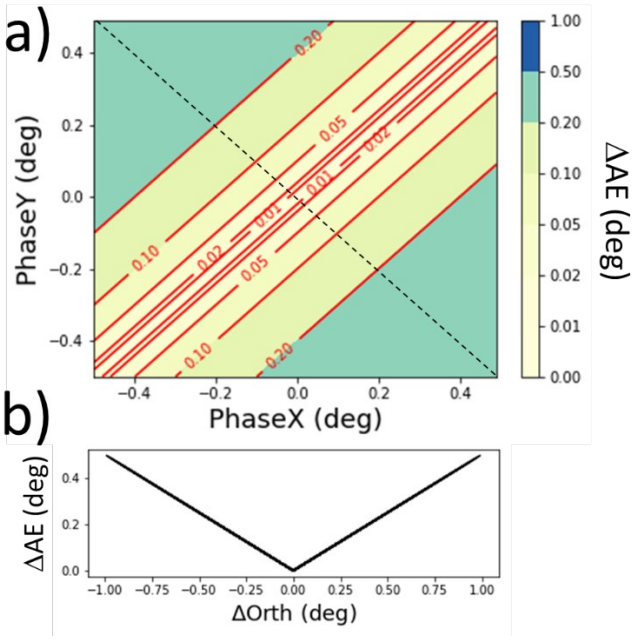

Figure 6: a) Increase of AE due to phase shift increase on both bridges. Dashed lines show increase of non-orthogonality. b) ΔAE vs. ΔOrth.

Parameter Increase	ΔAE (°)	Harmonic Contribution
Sync	0.29°/0.01	2nd
Total Offset	0.6°/%	1st
Orth	0.5°/°	2nd

Table 1: ΔAE ratio for each parameter increase and its harmonic contribution to AE.

These equations show that no possible cancelation of AE can be obtained by the combination of all three contributions. However, it also implies that the total AE induced by a combination of such three contributions will always be smaller than the addition of each individual contribution. Figure 7d shows the total AE obtained when combining all three contributions (Figures 7a, 7b and 7c) is ~ 1.16° which is smaller than 0.57° + 0.57° + 0.50° = 1.64°. Note that Figure 7d can be obtained either by calculating the total AE from Eq. 6a and Eq. 6b or by adding Eq. (A), Eq (B) and Eq. (C).

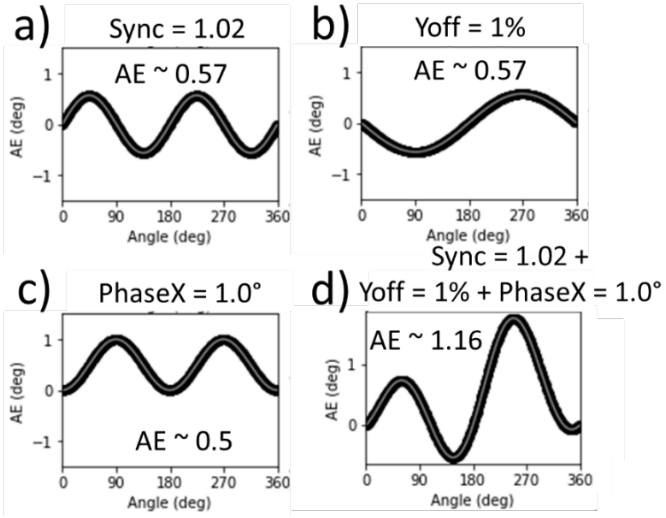

Figure 7: Angular dependence of AE for a) Sync = 1.02, C_{COS} = C_{SIN} = 0 and α_{COS} = α_{SIN} = 0; b) Sync = 1.0, C_{SIN}/A_{SIN} = 1%, C_{COS} = 0 and α_{COS} = α_{SIN} = 0; c) Sync = 1.0, C_{COS} = C_{SIN} = 0, α_{SIN} = 0 and α_{COS} = 1.0°.

It is clear, therefore, that mismatched amplitudes (or synchronism) and offsets of V_{OUT} as well as non-orthogonality between both bridges can have a big impact on AE. The following proposed correction methods will enable to rectify such contributions to improve accuracy on angle determination.

Method 1: AENorm

This method (also called "normalization correction") consists on the subtraction of the offset and normalization of the output voltage of each bridge. By this, a V_{COS}^{norm} and V_{SIN}^{norm} are obtained:

$$V_{COS}^{norm} = (V_{COS} - C_{COS})/A_{COS} \qquad Eq(8a)$$

$$V_{SIN}^{norm} = (V_{SIN} - C_{SIN})/A_{SIN} \qquad Eq(8b)$$

Which means, by considering Eq. 6a and 6b, that:

$$V_{COS}^{norm} = cos(\theta + \alpha_{COS}) \qquad Eq(9a)$$
$$V_{SIN}^{norm} = sin(\theta + \alpha_{SIN}) \qquad Eq(9b)$$

Thus, the measured angle will be determined by the arc tangent ratio between V_{SIN}^{norm} and V_{COS}^{norm} :

$$\theta_{meas}^{norm} = arctan\left(\frac{V_{SIN}^{norm}}{V_{COS}^{norm}}\right) \qquad Eq\ (10)$$

and the normalized Angular Error (AENorm) would be:

$$\text{AENorm} = \theta_{meas}^{norm} - \theta \qquad Eq\ (11)$$

This correction method would only require a first calibration procedure consisting on performing a unique rotational loop measurement. Then, by determining the maximum and minimum output voltages for each bridge A_{COS}^0, A_{SIN}^0 C_{COS}^0 and C_{SIN}^0 can be determined:

$$A_{COS}^0 = \left(V_{COS}^{max} - V_{COS}^{min}\right)/2 \qquad Eq\ (12a)$$

$$C_{COS}^0 = \left(V_{COS}^{max} + V_{COS}^{min}\right)/2 \qquad Eq\ (12b)$$

$$A_{SIN}^0 = \left(V_{SIN}^{max} - V_{SIN}^{min}\right)/2 \qquad Eq\ (12c)$$

$$C_{SIN}^0 = \left(V_{SIN}^{max} + V_{SIN}^{min}\right)/2 \qquad Eq\ (12d)$$

Such A_{COS}^0, A_{SIN}^0 C_{COS}^0 and C_{SIN}^0 parameters will then be used as parameter corrections of all measured data (V_{COS} and V_{SIN}) so:

$$V_{COS}^{norm} = \left(V_{COS} - C_{COS}^0\right)/A_{COS}^0 \qquad Eq(13a)$$

$$V_{SIN}^{norm} = \left(V_{SIN} - C_{SIN}^0\right)/A_{SIN}^0 \qquad Eq(13b)$$

and the measured angle will be determined by Eq.10.

Important improvements on AE can be obtained when considering the normalization of output voltages as observed in Figure 8. In this case, similar contributions of Sync, offset and phase shift as observed in Figure 7d are considered. By this correction method, reduction of AE from ~1.16° (black curve) to ~ 0.5° (red curve) is obtained.

Method 2: AECorr

Large reduction of AE can be obtained by normalization calibration (AENorm). However, possible contribution on AE from non-orthogonality can still be present as observed in Figure 8 (see red curve). Indeed, in such a case a non-orthogonality of 1.0° leads to an AENorm ~ 0.5°.

In order to remove such an effect, we need to expand Eq. 9a and Eq 9b:

$$V_{COS}^{norm} = cos\theta \cdot cos\alpha_{COS} - sin\theta \cdot sin\alpha_{COS} \qquad Eq(12a)$$

$$V_{SIN}^{norm} = sin\theta \cdot cos\alpha_{SIN} + cos\theta \cdot sin\alpha_{SIN} \qquad Eq(12b)$$

Then, considering small orthogonality deviations (i.e. small phase shifts α_{COS} and α_{SIN} → 0°) we obtain that:

$$V_{COS}^{norm} \sim cos\theta - \alpha_{COS} \cdot sin\theta \qquad Eq\ (13a)$$

$$V_{SIN}^{norm} \sim sin\theta + \alpha_{SIN} \cdot cos\theta \qquad Eq\ (13b)$$

This, can be expressed in the following matrix form:

$$\begin{bmatrix} V_{SIN}^{norm} \\ V_{COS}^{norm} \end{bmatrix} = \begin{bmatrix} 1 & \alpha_{SIN} \\ -\alpha_{COS} & 1 \end{bmatrix} \cdot \begin{bmatrix} sin\theta \\ cos\theta \end{bmatrix} \qquad Eq\ (14)$$

Then, by inverting this system of matrix equations and keeping only linear terms of α_{COS} and α_{SIN}, we have:

$$\begin{bmatrix} sin\theta \\ cos\theta \end{bmatrix} = \begin{bmatrix} 1 & -\alpha_{SIN} \\ \alpha_{COS} & 1 \end{bmatrix} \cdot \begin{bmatrix} V_{SIN}^{norm} \\ V_{COS}^{norm} \end{bmatrix} \qquad Eq(15)$$

Which is equivalent to:

$$sin\theta \sim V_{SIN}^{norm} - \alpha_{SIN} \cdot V_{COS}^{norm} \qquad Eq\ (16a)$$

$$cos\theta \sim \alpha_{COS} \cdot V_{SIN}^{norm} + V_{COS}^{norm} \qquad Eq\ (16b)$$

Thus, the measured angle will be determined by:

$$\theta_{meas}^{corr} = arctan\left(\frac{V_{SIN}^{norm} - \alpha_{SIN} \cdot V_{COS}^{norm}}{\alpha_{COS} \cdot V_{SIN}^{norm} + V_{COS}^{norm}}\right) \qquad Eq\ (17)$$

And the corrected Angular Error (AECorr) will be described as:

$$\text{AECorr} = \theta_{meas}^{corr} - \theta \qquad Eq\ (18)$$

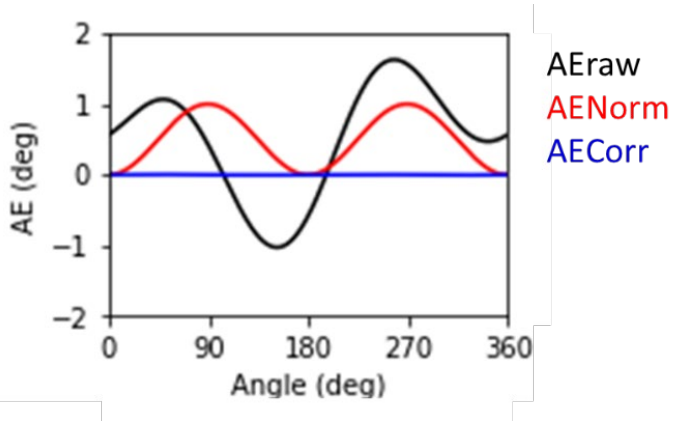

Figure 8: Angular dependence of AE for 2D sensor with Sync = 1.02, C_{SIN}/A_{SIN} = 1% and α_{COS} = 1.0°. AEraw (black curve) refers to the AE derived without any correction method. AENorm (red curve) refers to the AE derived from normalization correction and AECorr (blue curve) refers to the AE derived from non-orthogonality correction method.

This correction method (also called "non-orthogonality correction") requires, like normalization correction method, a first calibration procedure consisting on performing a unique rotational loop measurement. After this measurement, and in order to derive all required parameters (A_{COS}^0, A_{SIN}^0 C_{COS}^0 and C_{SIN}^0, α_{COS}^0 and α_{SIN}^0) both V_{COS} and V_{SIN} data need to be fitted following Eq. 6a and Eq. 6b. Then considering such parameters as parameter corrections for all next measured data (V_{COS} and V_{SIN}) the measured angle can therefore be determined by Eq. 8a, Eq. 8b and Eq. 17.

Complete reduction of AE can be achieved by this correction method. Figure 8 shows the performance of "non-orthogonality correction" to reduce AE ~ 0° (blue curve) in comparison to previous "normalization correction" (red curve).

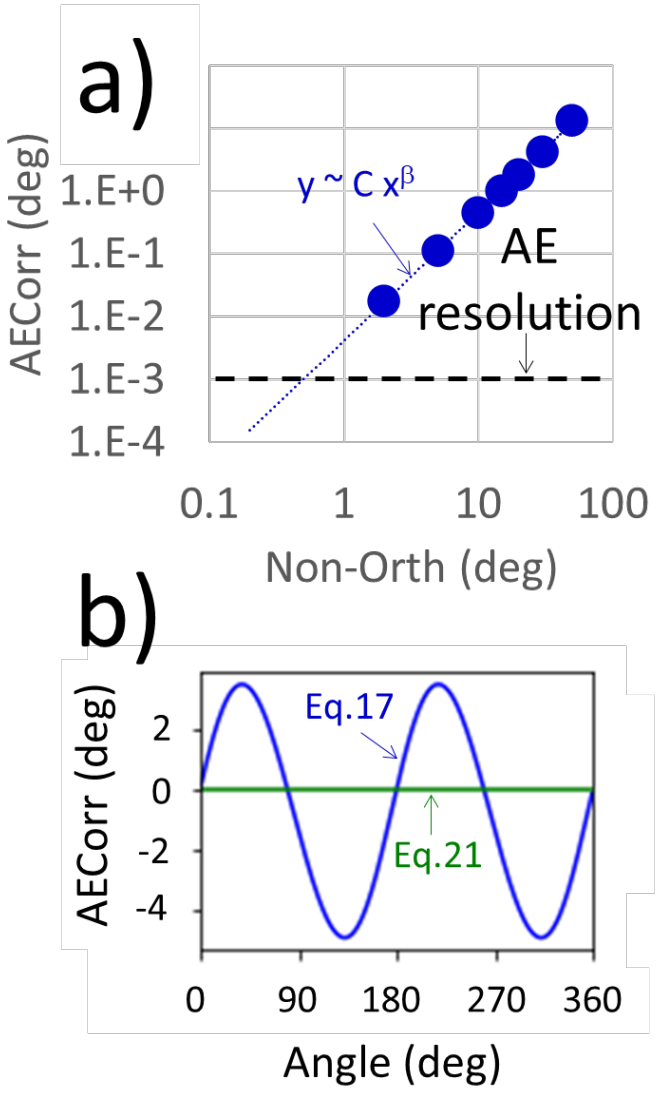

Figure 9: a) AECorr (determined by Eq. 17) vs. non-orthogonality. Black dashed lines indicate the usual AE resolution in a 2D magnetic sensor. C ~ 0.0041 and β ~ 2.04; b) angular dependence of AECorr with non-orthogonality of 30° when determining AECorr by Eq. 17 (blue curve) or by Eq. 21 (green curve).

As a matter of fact, Eq. 17 enables AE corrections for non-orthogonality values up to 2°. Figure 9a shows AECorr derived from Eq. 17 for a large range of non-orthogonality values showing almost a quadratic dependence. Thus, for a non-orthogonality < 1°, an

AECorr as low as 0.001° could be obtained, which is close to the maximum AE resolution such sensors usually hold. However, in case that unusually large non-orthogonality values (>5°) were present, a more general expression would be necessary to consider.

Indeed, Eq. 12a and Eq. 12b can expressed in the following matrix form:

$$\begin{bmatrix} V_{SIN}^{norm} \\ V_{COS}^{norm} \end{bmatrix} = \begin{bmatrix} cos\alpha_{SIN} & sin\alpha_{SIN} \\ -sin\alpha_{COS} & cos\alpha_{COS} \end{bmatrix} \cdot \begin{bmatrix} sin\theta \\ cos\theta \end{bmatrix} \quad Eq(19)$$

Then, by inverting this system of matrix equations, we have:

$$\begin{bmatrix} sin\theta \\ cos\theta \end{bmatrix} = \frac{1}{K} \begin{bmatrix} cos\alpha_{COS} & -sin\alpha_{SIN} \\ sin\alpha_{COS} & cos\alpha_{SIN} \end{bmatrix} \cdot \begin{bmatrix} V_{SIN}^{norm} \\ V_{COS}^{norm} \end{bmatrix} Eq(20)$$

With:

$$K = cos(\alpha_{SIN} - \alpha_{COS})$$

Thus, the measured angle will be determined by:

$$\theta_{meas}^{corr} = arctan\left(\frac{cos\alpha_{COS} \cdot V_{SIN}^{norm} - sin\alpha_{SIN} \cdot V_{COS}^{norm}}{sin\alpha_{COS} \cdot V_{SIN}^{norm} + cos\alpha_{SIN} \cdot V_{COS}^{norm}}\right) \quad Eq\ (21)$$

Figure 9b shows that such generalized non-orthogonal correction method enables to reduce AE ~ 0° (see green curve) even for a non-orthogonality of ~30°.

Therefore, in general, "non-orthogonality correction" enables to achieve higher angle accuracy than "normalized correction" without adding much complexity on the one-step calibration operation.

Stability of Correction

After such corrections, all 2D magnetic sensors will be able to guarantee an AENom < $AENorm_0$ (being $AENorm_0$ the max. AE after "normalization correction") or an AECorr < $AECorr_0$ (being $AECorr_0$ the max. AE after "non-orthogonality correction").

Moreover, the parameters derived from the one-step calibration procedure in both correction methods (A_{COS}^0, A_{SIN}^0 C_{COS}^0 and C_{SIN}^0 for "normalization correction" or A_{COS}^0, A_{SIN}^0 C_{COS}^0 and C_{SIN}^0, α_{COS}^0 and α_{SIN}^0 for "non-orthogonality correction") will be used during the whole lifetime of the sensor. This implies that such correction methods need to be stable for all working conditions, in other words, AENorm (or aAECorr) need to be stable for a certain temperature and magnetic field range.

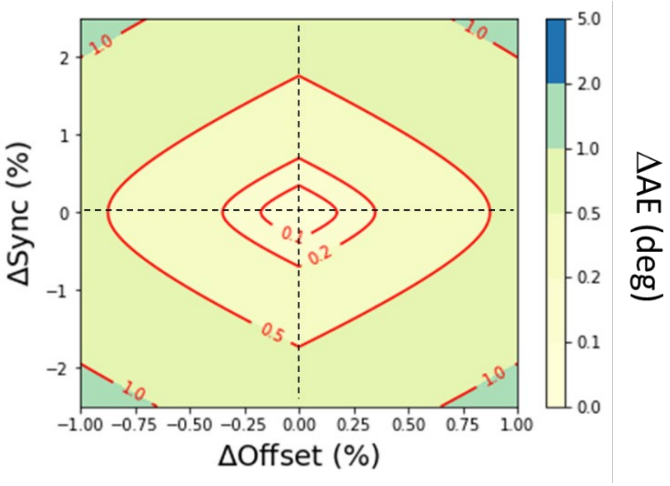

Figure 10: ΔAE map vs. ΔSync and ΔOffset. Here non-orthogonality was considered (α_{COS} and α_{SIN} = 0).

In order to guarantee this, it is important to ensure a minimum variation of synchronism, offset and orthogonality under such working conditions. Figure 10 shows a map of ΔAE vs. variation of ΔSync and ΔOffset. The contour lines of constant ΔAE follow a "diamond-like" shape. This map enables, therefore, to determine all possible variations of Sync and Offset that a 2D magnetic sensor could experience in order to guarantee an increase of AE below a certain level. Thus, for instance, if we want to ensure that after one-step calibration our sensors have a maximum

increase of ΔAENorm < 0.1° with temperature, it would be necessary, according to Figure 10, that ΔSync < 0.3% and ΔOffset < 0.6% (see stars on Figure 10).

Note, that similar conclusion could also be obtained from Table I being therefore very useful to quickly determine the maximum variation of Sync, total offset, and orthogonality for a certain increase of AE (ΔAE).

Similar analysis can also be done for non-orthogonality correction method which would enable to determine the max. variation of all three parameters to ensure a stable AECorr.

To conclude, stability of synchronism, offset and orthogonality are therefore crucial to ensure such calibration methods as a one-step calibration process that would be used during the whole lifetime of the sensor

Summary

Amplitude mismatch (synchronism), offset and non-orthogonality between both Wheatstone bridges impact the accuracy of the measured angle in 2D sensors. Several correction methods to minimize the AE induced by such parameters have been presented here.

The first method relies on normalization of measured voltages enabling to remove synchronism and offset contributions. This simple technique requires one-time calibration operation and basic calculation computation. After correction parameters derived, they are used for rectification of all subsequent measurements. This method, however, does not correct non-orthogonality contributions on AE.

The second method relies on complete correction (amplitude mismatch, offset and non-orthogonality) of measured voltages by a fitting procedure. This technique requires also one-time calibration operation with only one additional calculation step with respect to normalization correction. After correction parameters derived, subsequent measurements are rectified by using such parameters

By such corrections, the maximum AE of the 2D magnetic sensor can substantially be reduced improving the accuracy of the measured angle.

Both correction methods rely on the stability of synchronism, offset and non-orthogonality with respect other parameters like temperature and magnetic field.